

Research Article

NUMERICAL SOLUTION OF AN UNSTEADY MHD FLOW ALONG A FLAT PLATE WITH VISCOUS DISSIPATION AND HALL CURRENT

***Anitha K.**

*Department of BS&H, BVRITH College of Engineering for Women,
 Bachupally, Hyderabad -90, India*

**Author for Correspondence*

ABSTRACT

The effect of Hall current on MHD flow of an electrically conducting incompressible fluid along an infinite vertical porous plate with viscous dissipation and heat absorption has been studied. The problem is solved, numerically by Galerkin finite element method for velocity, temperature, concentration field and also the expression for shearing stress, Rate of heat transfer and mass transfer is obtained. The effect of Grashof Number, Modified Grashof Number, Transpiration cooling parameter, Prandtl Number, Schmidt Number, Eckert number, Hartmann number, Heat absorption parameter and Hall parameter on the flow field are shown through graphs and tables.

Keywords: *MHD Flow, Free Convection, Hall Current, Heat Transfer, Mass Transfer, Galerkin Finite Element Method*

Nomenclature

C'	Dimensionless concentration	ε	Porosity of the porous medium
C_w	Concentration near the plate	C_∞	Concentration in the fluid far away from the plate
θ	Dimensionless Temperature	T_w	Temperature of the plate
T	Temperature of the fluid	u'	Velocity component in x' - direction
T_∞	Temperature of the fluid far away from the plate	x'	Spatial co – ordinate along the plate
w'	Velocity component in z' - direction	α	Thermal Diffusivity
ν	Kinematics viscosity, m^2/s	\bar{V}	Velocity vector, m/s
y'	Spatial co – ordinate normal to the plate	m	Hall parameter
k_e	Mean absorption coefficient	μ	Viscosity, Ns/m^2
k	Thermal conductivity, W/mK	C_p	Specific heat at constant Pressure, J/kg-K
σ	Electrical conductivity, mho/m	D	Chemical molecular diffusivity
μ_e	Magnetic permeability, Henry/meter	U_o	Reference velocity
ρ	Density, kg/m^3	M	Hartmann number
ω_e	Electron frequency, radian/sec	Pr	Prandtl number
τ_e	Electron collision time in Sec	Sc	Schmidt Number
e	Electron charge, coulombs	Gr	Grashof Number
n_e	Number density of the electron	Ec	Eckert number
P_e	Electron Pressure, N/ m^2	Gc	Modified Grashof Number
g	Acceleration due to Gravity, $9.81 m/s^2$		
β	Volumetric co – efficient of thermal expansion		

Research Article

β^* Co – efficient of volume expansion
with Species concentration

λ Non – dimensional transpiration
parameter

INTRODUCTION

The phenomenon of free convection arises in the fluid when temperature changes cause density variation leading to buoyancy forces acting on the fluid elements. This can be seen in our everyday life in the atmospheric flow, which is driven by temperature differences. Incompressible viscous fluids over and through a porous medium has a wide variety of applications in the field of agricultural sciences, chemical engineering and petroleum technology. Considerable attention has been given to the unsteady free convection flow of viscous incompressible, electrically conducting fluid in presence of applied magnetic field in connection with the theories of fluid motion in the liquid core of the Earth and also meteorological and oceanographic applications. In geophysics, it finds its applications in the design of MHD generators and accelerators, underground water energy storage system etc. It is worth – mentioning that MHD is now undergoing a stage of great enlargement and differentiation of subject matter. These new problems draw the attention of the researchers due to their varied significance, in liquid metals, electrolytes and ionized gases etc. In addition, the applications of the effect of Hall current on the fluid flow with variable concentration have been seen in MHD power generators, astrophysical and meteorological studies as well as in plasma physics. The Hall Effect is due merely to the sideways magnetic force on the drifting free charges. The electric field has to have a component transverse to the direction of the current density to balance this force. In many works on plasma physics, the Hall Effect is disregarded. But if the strength of magnetic field is high and the number density of electrons is small, the Hall Effect cannot be ignored as it has a significant effect on the flow pattern of an ionized gas. Hall Effect results in a development of an additional potential difference between opposite surfaces of a conductor for which a current is induced perpendicular to both the electric and magnetic field. This current is termed as Hall current. Model studies on the effect of Hall current on MHD convection flows have been carried out by many authors due to application of such studies in the problems of MHD generators and Hall accelerators.

From the point of view of applications, this effect can be taken into account within the range of Magnetohydrodynamical approximation. Abdul and Abdur *et al.*, (2005) studied the effects of variable properties and Hall current on steady MHD laminar convective fluid flow due to a porous rotating disk. Ajay (2003) made an attempt to study the steady MHD free convection and mass transfer flow with hall current, viscous dissipation and joule heating, taking in to account the thermal diffusion effect. Anand and Srinivasa *et al.*, (2010) investigated applied magnetic field on transient free convective flow of an incompressible viscous dissipative fluid in a vertical channel. Anand and Srinivasa (2011) studied the effect of hall current on an unsteady magnetohydrodynamic flow past along a porous flat plate with heat and mass transfer in presence of viscous dissipation by. Anjali *et al.*, (2011) discussed pulsated convective MHD flow with Hall current, heat source and viscous dissipation along a vertical porous plate. Atul *et al.*, (2005) studied hydromagnetic free convection and mass transfer flow with Joule heating, thermal diffusion, Heat source and Hall current. Chowdhary and Kumar (2008) studied heat and mass transfer in elasticoviscous fluid past an impulsively started infinite vertical plate with Hall Effect. Chaudhary and Jain (2007) analyzed Hall Effect on MHD mixed convection flow of a viscoelastic fluid past an infinite vertical porous plate with mass transfer and radiation. On the effectiveness of viscous dissipation and Joule heating on steady MHD and slip flow of a bingham fluid over a porous rotating disk in the presence of Hall and ion – slip currents was studied by Emmanuel *et al.*, (2009).

Hossain and Rashid (1987) investigated the effect of hall current on the unsteady free convection flow of a viscous incompressible fluid with heat and mass transfer along a vertical porous plate subjected to a time dependent transpiration velocity when the constant magnetic field is applied normal to the flow. MHD stationary symmetric flows with Hall effect was analyzed by Palumbo and Platzack (2006). Rajashekhar *et al.*, (1999) studied the effect of hall current on free convection and mass transfer flow through a porous medium bounded by an infinite vertical porous plate, when the plate was subjected to a constant suction velocity and heat flux. Singh (1996) studied the effects of mass transfer on the flow past

Research Article

a vertical porous plate. Singh *et al.*, (1996) analyzed the free convection heat and mass transfer along a vertical surface in a porous medium. Later, Soundalgekar *et al.*, (1995) studied the coupled heat and mass transfer by natural convection from vertical surfaces in a porous medium. Hall Effect on MHD Flow and Heat Transfer along a Porous Flat Plate with Mass Transfer and Source/Sink was analyzed by Srihari *et al.*, (2008). Sriramulu *et al.*, (2007) discussed the effect of Hall Current on MHD flow and heat transfer along a porous flat plate with mass transfer.

In this paper we studied the Hall Effect on MHD flow and mass transfer of an electrically conducting incompressible fluid along an infinite vertical porous plate with viscous dissipation. Also, the effects of different flow parameters encountered in the equations are studied. The results obtained are good agreement with the results of Sriramulu *et al.*, (2007). The problem is governed by system of coupled non – linear partial differential equations whose exact solution is difficult to obtain. Hence, the problem is solved by using Galerkin finite element method, which is more economical from computational view point.

Mathematical Analysis

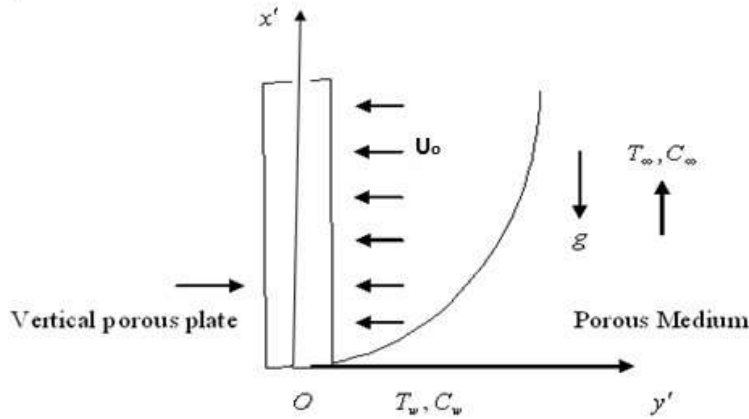


Figure 1: Physical sketch and geometry of the problem

An unsteady free convection flow of an electrically conducting viscous incompressible fluid with mass transfer along a porous flat plate has been considered with viscous dissipation. The flow is assumed to be in x' – direction, which is taken along the plate in upward direction. The y' – direction which is taken along the normal to the direction of the plate. Initially, for time $t' \leq 0$, the plate and the fluid are maintained at the same constant temperature T_∞ in a stationary condition with the same species concentration C_∞ at all points so that, the Soret and Dufour effects are neglected. When $t' > 0$, the temperature of the plate is instantaneously raised (or lowered) to T_w and the concentration of the species is raised (or lowered) to C_w , which are hereafter regarded as constant. We also assumed that the level of species concentration is very low and hence species thermal diffusion and diffusion thermal energy effects can be neglected. A magnetic field of uniform strength is assumed to be applied transversely to the porous plate. The magnetic Reynolds number of the flow is taken to be small enough so that the induced magnetic field can be neglected.

Using the relation $\nabla \cdot \bar{H} = 0$ for the magnetic field $\bar{H} = (H_x, H_y, H_z)$, we obtain $H_y = \text{constant} = H_o$ (say) where H_o is the externally applied transverse magnetic field so that $\bar{H} = (0, H_o, 0)$. The equation of conservation of electric charge $\nabla \cdot \bar{J} = 0$ gives $j_y = \text{constant}$, where $\bar{J} = (j_x, j_y, j_z)$. We further assume that the plate is non – conducting. This implies $j_y = 0$ at the plate and hence zero everywhere.

Research Article

When the strength of magnetic field is very large, the generalized Ohm's law in the absence of electric field takes the following form:

$$\bar{J} + \frac{\omega_e \tau_e}{B_o} \bar{J} \times \bar{H} = \sigma \left(\mu_e \bar{V} \times \bar{H} + \frac{1}{en_e} \nabla P_e \right) \quad (1)$$

Under the assumption that the electron pressure (for weakly ionized gas), the thermo – electric pressure and ion – slip conditions are negligible, equation (1) becomes:

$$j_x = \frac{\sigma \mu_e H_o}{1+m^2} (mu' - w') \text{ and } j_z = \frac{\sigma \mu_e H_o}{1+m^2} (mw' + u') \quad (2)$$

Where u' is the x' – component of \bar{V} , w' is the z' – component of \bar{V} and $m (= \omega_e \tau_e)$ is the hall parameter. Within the above framework, the equations which govern the flow under the usual Boussinesq's approximation are as follows:

$$\frac{\partial v'}{\partial y'} = 0 \quad (3)$$

$$\frac{\partial u'}{\partial t'} + v' \frac{\partial u'}{\partial y'} = \nu \frac{\partial^2 u'}{\partial y'^2} - \frac{\sigma \mu_e^2 H_o^2}{\rho(1+m^2)} (u' + mw') + g\beta(T - T_\infty) + g\beta^*(C' - C_\infty) \quad (4)$$

$$\frac{\partial w'}{\partial t'} + v' \frac{\partial w'}{\partial y'} = \nu \frac{\partial^2 w'}{\partial y'^2} - \frac{\sigma \mu_e^2 H_o^2}{\rho(1+m^2)} (w' - mu') \quad (5)$$

$$\frac{\partial T}{\partial t'} + v' \frac{\partial T'}{\partial y'} = \frac{k}{\rho c_p} \frac{\partial^2 T}{\partial y'^2} + \frac{\nu}{c_p} \left(\frac{\partial u'}{\partial y'} \right)^2 \quad (6)$$

$$\frac{\partial C}{\partial t'} + v' \frac{\partial C'}{\partial y'} = D \frac{\partial^2 C'}{\partial y'^2} \quad (7)$$

The initial and boundary conditions of the problem are:

$$t' \leq 0: u' = 0, w' = 0, T = T_\infty, C' = C_\infty \text{ for all } y'$$

$$t' > 0: \begin{cases} u' = 0, w' = 0, T = T_w, C' = C_w \text{ at } y' = 0 \\ u' = 0, w' = 0, T = T_\infty, C' = C_\infty \text{ as } y' \rightarrow \infty \end{cases} \quad (8)$$

The non – dimensional quantities introduced in the equations (3) – (7) are:

$$\left. \begin{aligned} t &= \frac{t' U_o^2}{\nu}, \quad y = \frac{y' U_o}{\nu}, \quad (u, v, w) = \frac{(u', v', w')}{U_o}, \quad \theta = \frac{(T - T_\infty)}{(T_w - T_\infty)}, \\ C &= \frac{(C' - C_\infty)}{(C_w - C_\infty)}, \quad M = \frac{\sigma \mu_e^2 H_o^2 \nu}{\rho U_o^2}, \quad Pr = \frac{\mu C_p}{k}, \quad Ec = \frac{U_o^2}{C_p (T_w - T_\infty)}, \\ Sc &= \frac{\nu}{D}, \quad Gr = \frac{\nu g \beta (T_w - T_\infty)}{U_o^3}, \quad Gc = \frac{\nu g \beta^* (C_w - C_\infty)}{U_o^3} \end{aligned} \right\} \quad (9)$$

Where U_o is the reference velocity. The governing equations can be obtained in the dimensionless form as:

Research Article

$$\frac{\partial v}{\partial y} = 0 \tag{10}$$

$$\frac{\partial u}{\partial t} + v \frac{\partial u}{\partial y} = \frac{\partial^2 u}{\partial y^2} - \frac{M}{(1+m^2)}(u+mw) + (Gr)\theta + (Gc)C \tag{11}$$

$$\frac{\partial w}{\partial t} + v \frac{\partial w}{\partial y} = \frac{\partial^2 w}{\partial y^2} - \frac{M}{(1+m^2)}(w-mu) \tag{12}$$

$$\frac{\partial \theta}{\partial t} + v \frac{\partial \theta}{\partial y} = \frac{1}{Pr} \frac{\partial^2 \theta}{\partial y^2} + (Ec) \left(\frac{\partial u}{\partial y} \right)^2 \tag{13}$$

$$\frac{\partial C}{\partial t} + v \frac{\partial C}{\partial y} = \frac{1}{Sc} \frac{\partial^2 C}{\partial y^2} \tag{14}$$

The initial and boundary conditions (8) in the non – dimensional form are:

$$\left. \begin{aligned} t \leq 0: & \quad u = 0, w = 0, \theta = 0, C = 0 \quad \text{for all } y \\ t > 0: & \quad \left\{ \begin{aligned} u = 0, w = 0, \theta = 1, C = 1 & \quad \text{at } y = 0 \\ u = 0, w = 0, \theta = 0, C = 0 & \quad \text{as } y \rightarrow \infty \end{aligned} \right\} \end{aligned} \right\} \tag{15}$$

From equation (10), we see that v is either constant or a function of time t . Similarly solutions of equations (11) – (14) with the boundary conditions (15) exists only if we take

$$v = \lambda t^{-\frac{1}{2}} \tag{16}$$

where λ is a non – dimensional transpiration parameter. For suction $\lambda > 0$ and for blowing $\lambda < 0$. From (16), it can be observed that the assumption is valid only for small values of time variable.

Method of Solution

By applying Galerkin finite element method for equation (11) over the element (e), $(y_j \leq y \leq y_k)$

is:

$$\int_{y_j}^{y_k} \left\{ N^{(e)T} \left[\frac{\partial^2 u^{(e)}}{\partial y^2} - \frac{\partial u^{(e)}}{\partial t} - v \frac{\partial u^{(e)}}{\partial y} - Au^{(e)} + P \right] \right\} dy = 0 \tag{17}$$

where $A = \frac{M}{1+m^2}$, $P = (Gr)\theta_i^j + (Gc)C_i^j - Amw_i^j$

Integrating the first term in equation (17) by parts one obtains

$$N^{(e)T} \left\{ \frac{\partial u^{(e)}}{\partial y} \right\}_{y_j}^{y_k} - \int_{y_j}^{y_k} \left\{ \frac{\partial N^{(e)T}}{\partial y} \frac{\partial u^{(e)}}{\partial y} + N^{(e)T} \left(\frac{\partial u^{(e)}}{\partial t} + v \frac{\partial u^{(e)}}{\partial y} + Au^{(e)} - P \right) \right\} dy = 0 \tag{18}$$

Neglecting the first term in equation (18), one gets:

Let $u^{(e)} = N^{(e)}\phi^{(e)}$ be the linear piecewise approximation solution over the element (e) $(y_j \leq y \leq y_k)$, where $N^{(e)} = [N_j \quad N_k]$, $\phi^{(e)} = [u_j \quad u_k]^T$ and $N_j = \frac{y_k - y}{y_k - y_j}$, $N_k = \frac{y - y_j}{y_k - y_j}$ are the basis functions. One obtains:

Research Article

$$\int_{y_j}^{y_k} \left\{ \begin{bmatrix} N'_j & N'_j & N'_j & N'_k \\ N'_j & N'_k & N'_k & N'_k \end{bmatrix} \begin{bmatrix} u_j \\ u_k \end{bmatrix} \right\} dy + \int_{y_j}^{y_k} \left\{ \begin{bmatrix} N_j & N_j & N_j & N_k \\ N_j & N_k & N_k & N_k \end{bmatrix} \begin{bmatrix} \dot{u}_j \\ \dot{u}_k \end{bmatrix} \right\} dy + \nu \int_{y_j}^{y_k} \left\{ \begin{bmatrix} N_j & N'_j & N_j & N'_k \\ N'_j & N_k & N'_k & N_k \end{bmatrix} \begin{bmatrix} u_j \\ u_k \end{bmatrix} \right\} dy$$

$$+ A \int_{y_j}^{y_k} \left\{ \begin{bmatrix} N_j & N_j & N_j & N_k \\ N_j & N_k & N_k & N_k \end{bmatrix} \begin{bmatrix} u_j \\ u_k \end{bmatrix} \right\} dy = P \int_{y_j}^{y_k} \begin{bmatrix} N_j \\ N_k \end{bmatrix} dy$$

Simplifying we get

$$\frac{1}{l^{(e)^2}} \begin{bmatrix} 1 & -1 \\ -1 & 1 \end{bmatrix} \begin{bmatrix} u_j \\ u_k \end{bmatrix} + \frac{1}{6} \begin{bmatrix} 2 & 1 \\ 1 & 2 \end{bmatrix} \begin{bmatrix} \dot{u}_j \\ \dot{u}_k \end{bmatrix} + \frac{\nu}{2l^{(e)}} \begin{bmatrix} -1 & 1 \\ -1 & 1 \end{bmatrix} \begin{bmatrix} u_j \\ u_k \end{bmatrix} + \frac{A}{6} \begin{bmatrix} 2 & 1 \\ 1 & 2 \end{bmatrix} \begin{bmatrix} u_j \\ u_k \end{bmatrix} = \frac{P}{2} \begin{bmatrix} 1 \\ 1 \end{bmatrix}$$

Using the above equation, in order to get the difference equation at the nodes $(y_{i-1} \leq y \leq y_i)$ and $(y_i \leq y \leq y_{i+1})$. We write the element equation for the element $(y_{i-1} \leq y \leq y_i)$ as

$$\frac{1}{l^{(e)^2}} \begin{bmatrix} 1 & -1 \\ -1 & 1 \end{bmatrix} \begin{bmatrix} u_{i-1} \\ u_i \end{bmatrix} + \frac{1}{6} \begin{bmatrix} 2 & 1 \\ 1 & 2 \end{bmatrix} \begin{bmatrix} \dot{u}_{i-1} \\ \dot{u}_i \end{bmatrix} + \frac{\nu}{2l^{(e)}} \begin{bmatrix} -1 & 1 \\ -1 & 1 \end{bmatrix} \begin{bmatrix} u_{i-1} \\ u_i \end{bmatrix} + \frac{A}{6} \begin{bmatrix} 2 & 1 \\ 1 & 2 \end{bmatrix} \begin{bmatrix} u_{i-1} \\ u_i \end{bmatrix} = \frac{P}{2} \begin{bmatrix} 1 \\ 1 \end{bmatrix}$$

and for the second element $(y_i \leq y \leq y_{i+1})$ we get the element equation as

$$\frac{1}{l^{(e)^2}} \begin{bmatrix} 1 & -1 \\ -1 & 1 \end{bmatrix} \begin{bmatrix} u_i \\ u_{i+1} \end{bmatrix} + \frac{1}{6} \begin{bmatrix} 2 & 1 \\ 1 & 2 \end{bmatrix} \begin{bmatrix} \dot{u}_i \\ \dot{u}_{i+1} \end{bmatrix} + \frac{\nu}{2l^{(e)}} \begin{bmatrix} -1 & 1 \\ -1 & 1 \end{bmatrix} \begin{bmatrix} u_i \\ u_{i+1} \end{bmatrix} + \frac{A}{6} \begin{bmatrix} 2 & 1 \\ 1 & 2 \end{bmatrix} \begin{bmatrix} u_i \\ u_{i+1} \end{bmatrix} = \frac{P}{2} \begin{bmatrix} 1 \\ 1 \end{bmatrix}$$

where prime and dot denotes differentiation w.r.t y and time t respectively. Assembling the above two element equations for two consecutive elements $(y_{i-1} \leq y \leq y_i)$ and $(y_i \leq y \leq y_{i+1})$ following is obtained:

$$\frac{1}{l^{(e)^2}} \begin{bmatrix} 1 & -1 & 0 \\ -1 & 2 & -1 \\ 0 & -1 & 1 \end{bmatrix} \begin{bmatrix} u_{i-1} \\ u_i \\ u_{i+1} \end{bmatrix} + \frac{1}{6} \begin{bmatrix} 2 & 1 & 0 \\ 1 & 4 & 1 \\ 0 & 1 & 2 \end{bmatrix} \begin{bmatrix} \dot{u}_{i-1} \\ \dot{u}_i \\ \dot{u}_{i+1} \end{bmatrix} + \frac{\nu}{2l^{(e)}} \begin{bmatrix} -1 & 1 & 0 \\ -1 & 0 & 1 \\ 0 & -1 & 1 \end{bmatrix} \begin{bmatrix} u_{i-1} \\ u_i \\ u_{i+1} \end{bmatrix}$$

$$+ \frac{A}{6} \begin{bmatrix} 2 & 1 & 0 \\ 1 & 4 & 1 \\ 0 & 1 & 2 \end{bmatrix} \begin{bmatrix} u_{i-1} \\ u_i \\ u_{i+1} \end{bmatrix} = \frac{P}{2} \begin{bmatrix} 1 \\ 2 \\ 1 \end{bmatrix} \tag{19}$$

Now put row corresponding to the node i to zero, from equation (19) the difference schemes with $l^{(e)} = h$ is:

$$\frac{1}{h^2} [-u_{i-1} + 2u_i - u_{i+1}] + \frac{1}{6} \begin{bmatrix} \dot{u}_{i-1} + 4\dot{u}_i + \dot{u}_{i+1} \end{bmatrix} + \frac{\nu}{2h} [-u_{i-1} + u_{i+1}] + \frac{A}{6} [u_{i-1} + 4u_i + u_{i+1}] = P \tag{20}$$

Applying the trapezoidal rule, following system of equations in Crank – Nicholson method are obtained:

Research Article

$$A_1 u_{i-1}^{n+1} + A_2 u_i^{n+1} + A_3 u_{i+1}^{n+1} = A_4 u_{i-1}^n + A_5 u_i^n + A_6 u_{i+1}^n + 12Phk \quad (21)$$

Now from equations (12), (13) and (14), following equations are obtained:

$$B_1 w_{i-1}^{n+1} + B_2 w_i^{n+1} + B_3 w_{i+1}^{n+1} = B_4 w_{i-1}^n + B_5 w_i^n + B_6 w_{i+1}^n + 12hkAmu_i^j \quad (22)$$

$$G_1 \theta_{i-1}^{n+1} + G_2 \theta_i^{n+1} + G_3 \theta_{i+1}^{n+1} = G_4 \theta_{i-1}^n + G_5 \theta_i^n + G_6 \theta_{i+1}^n + 12hk(Pr)Ec \left(\frac{\partial u_i^j}{\partial y} \right)^2 \quad (23)$$

$$J_1 C_{i-1}^{n+1} + J_2 C_i^{n+1} + J_3 C_{i+1}^{n+1} = J_4 C_{i-1}^n + J_5 C_i^n + J_6 C_{i+1}^n \quad (24)$$

Where $A_1 = 2h + Ahk - 3vk - 6rh$, $A_2 = 4Akh + 12rh + 8h$, $A_3 = 2h + Ahk + 3vk - 6rh$

$$A_4 = 2h - Ahk + 3vk - 6rh, A_5 = 8h - 4Akh - 12rh, A_6 = 2h - Ahk - 3vk + 6rh$$

$$B_1 = 2h + Ahk - 3vk - 6rh, B_2 = 4Akh + 12rh + 8h, B_3 = 2h + Ahk + 3vk - 6rh$$

$$B_4 = 2h - Ahk + 3vk - 6rh, B_5 = 8h - 4Akh - 12rh, B_6 = 2h - Ahk - 3vk + 6rh$$

$$G_1 = 2(Pr)h - 3v(Pr)k - 6rh + (Pr)hk, G_2 = 8(Pr)h + 12rh + 4(Pr)hk,$$

$$G_3 = 2(Pr)h + 3v(Pr)k - 6rh + (Pr)hk, G_4 = 2(Pr)h + 3v(Pr)k + 6rh - (Pr)hk,$$

$$G_5 = 8(Pr)h - 12rh - 4(Pr)hk, G_6 = 2(Pr)h - 3v(Pr)k + 6rh - (Pr)hk,$$

$$J_1 = 2(Sc)h - 3v(Sc)k - 6rh, J_2 = 8(Sc)h + 12rh, J_3 = 2(Sc)h + 3v(Sc)k - 6rh,$$

$$J_4 = 2(Sc)h + 3v(Sc)k + 6rh, J_5 = 8(Sc)h - 12rh, J_6 = 2(Sc)h - 3v(Sc)k + 6rh,$$

$$P = (Gr)\theta_i^j + (Gc)C_i^j - Amw_i^j$$

Here $r = \frac{k}{h^2}$ and h, k are mesh sizes along y - direction and t - direction respectively. Index i refers

to space and j refers to the time. In the equations (21), (22), (23) and (24) taking $i = 1(1)n$ and using boundary conditions (15), then the following system of equations are obtained:

$$A_i X_i = B_i \quad i = 1(1)4 \quad (25)$$

Where A_i 's are matrices of order n and X_i, B_i 's are column matrices having n - components. The solutions of above system of equations are obtained by using Thomas algorithm for primary velocity, secondary velocity, temperature and concentration. Also, numerical solutions for these equations are obtained by C - programme. In order to prove the convergence and stability of Galerkin finite element method, the same C - programme was run with smaller values of h and k and no significant change was observed in the values of u, w, θ and C . Hence the Galerkin finite element method is stable and convergent.

Shearing Stress, Rate of Heat and Mass Transfer

The skin - friction at the wall along x' - axis is given by $\tau_1 = \left(\frac{\partial u}{\partial y} \right)_{y=0}$

The skin - friction at the wall along z' - axis is given by $\tau_2 = \left(\frac{\partial w}{\partial y} \right)_{y=0}$

RESULTS AND DISCUSSION

The problem of Hall Effect on MHD flow and mass transfer of an electrically conducting incompressible fluid along an infinite vertical porous plate with viscous dissipation and heat absorption has been studied and solved by using Galerkin finite element method. The effects of material parameters such as Grashof number (Gr), Modified Grashof number (Gc) Prandtl number (Pr), Schmidt number (Sc), Hartmann

Research Article

number (M), Hall parameter (m), Eckert number (Ec) and Transpiration cooling parameter (λ) separately in order to clearly observe their respective effects on the primary velocity, secondary velocity, temperature and concentration profiles of the flow. And also numerical values of skin – friction coefficients (τ_1 & τ_2) have been discussed in table 1. We discussed the effects of material parameters on primary velocity profiles from figures (1) to (8), secondary velocity profiles from figures (9) to (16), temperature profiles from figures (17) to (19) and concentration profiles from the figures (20) and (21). During the course of numerical calculations of the primary velocity (u), secondary velocity (w), temperature (θ) and concentration (C) the values of the Prandtl number are chosen for Mercury ($Pr = 0.025$), Air at $25^\circ C$ and one atmospheric pressure ($Pr = 0.71$) and Water ($Pr = 7.00$). To focus out attention on numerical values of the results obtained in the study, the values of Sc are chosen for the gases representing diffusing chemical species of most common interest in air namely Hydrogen ($Sc = 0.22$), Helium ($Sc = 0.30$), Water – vapour ($Sc = 0.60$), Oxygen ($Sc = 0.66$) and Ammonia ($Sc = 0.78$). For the physical significance, the numerical discussions in the problem and at $t = 1.0$, stable values for primary velocity, secondary velocity, temperature and concentration fields are obtained. To examine the effect of parameters related to the problem on the velocity field and skin – friction numerical computations are carried out at $Pr = 0.71$. To find out the solution of this problem, we have placed an infinite vertical plate in a finite length in the flow. Hence, we solve the entire problem in a finite boundary. However, in the graphs, the y values vary from 0 to 4, and the velocity, temperature, and concentration tend to zero as y tends to 4. This is true for any value of y . Thus, we have considered finite length.

The temperature and the species concentration are coupled to the velocity via Grashof number (Gr) and Modified Grashof number (Gc) as seen in equation (11). For various values of Grashof number and Modified Grashof number, the velocity profiles u are plotted in figures (1) and (2). The Grashof number (Gr) signifies the relative effect of the thermal buoyancy force to the viscous hydrodynamic force in the boundary layer. As expected, it is observed that there is a rise in the velocity due to the enhancement of thermal buoyancy force. Also, as Gr increases, the peak values of the velocity increases rapidly near the porous plate and then decays smoothly to the free stream velocity. The Modified Grashof number (Gc) defines the ratio of the species buoyancy force to the viscous hydrodynamic force. As expected, the fluid velocity increases and the peak value is more distinctive due to increase in the species buoyancy force. The velocity distribution attains a distinctive maximum value in the vicinity of the plate and then decreases properly to approach the free stream value. It is noticed that the velocity increases with increasing values of Modified Grashof number (Gc). The nature of primary velocity profiles in presence of foreign species such as Hydrogen ($Sc = 0.22$), Oxygen ($Sc = 0.60$) and Ammonia ($Sc = 0.78$) are shown in figure (3). The flow field suffers a decrease in primary velocity at all points in presence of heavier diffusing species.

The influence of the viscous dissipation parameter i.e., the Eckert number (Ec) on the velocity and temperature are shown in figures (4) and (18) respectively. The Eckert number (Ec) expresses the relationship between the kinetic energy in the flow and the enthalpy. It embodies the conversion of kinetic energy into internal energy by work done against the viscous fluid stresses. Greater viscous dissipative heat causes a rise in the temperature as well as the velocity. This behavior is evident from figures (4) and (18). Figure (5) depicts the effect of Prandtl number on primary velocity profiles in presence of foreign species such as Mercury ($Pr = 0.025$), Air ($Pr = 0.71$) and Water ($Pr = 7.00$) are shown in figure (5). We observe that from figure (5), the primary velocity decreases with increasing of Prandtl number (Pr). The effect of the Hartmann number (M) is shown in figure (6). It is observed that, the primary velocity of the fluid decreases with the increasing of the magnetic field number values. The decrease in the primary

Research Article

velocity as the Hartmann number (M) increases is because the presence of a magnetic field in an electrically conducting fluid introduces a force called the Lorentz force, which acts against the flow, if the magnetic field is applied in the normal direction, as in the present study. This resistive force slows down the fluid velocity component as shown in figure (6).

Figure (7) depicts the primary velocity profiles as the Hall parameter m increases. We see that u increases as m increases. It can also be observed that u profiles approach their classical values when Hall parameter m becomes large ($m > 5$). From figure (8) shows that the primary velocity profiles against y for several values of the transpiration cooling parameter (λ) keeping other parameters of the flow field are constant. The transpiration cooling parameter is found to retard the primary velocity of the flow field at all points. The reduction in primary velocity at any point of the flow field is faster as the transpiration cooling parameter becomes larger. One interesting inference of this finding is greater transpiration cooling leads to a faster reduction in the primary velocity of the flow field.

In figure (16), we see that w profiles increase for $m < 1$ and decrease for $m > 1$. In figures (10) and (11), we see the influence of the both heat and mass transfer on secondary velocity of the flow. It can be seen that as both the heat and mass transfer increases, this velocity component increases as well. In figures (10) and (11), the effects of the heat and mass transfer on the velocity are displayed. It is apparent from the figures that, the increasing values of heat and mass transfer enhance the secondary velocity. The effect of Eckert number (Ec) on the secondary velocity flow field is presented in the figure (13). Here, the secondary velocity profiles are drawn against y for three different values of Ec . The Eckert number is found to accelerate the secondary velocity of the flow field at all points.

In figure (15) we have the influence of the Hartmann number (M) on the secondary velocity. It can be seen that as the values of this parameter increases, the secondary velocity increases. The nature of secondary velocity profiles in presence of foreign species such as H_2 ($Sc = 0.22$), O_2 ($Sc = 0.60$) and NH_3 ($Sc = 0.78$) are shown in figure (12).

The flow field suffers a decrease in secondary velocity at all points in presence of heavier diffusing species. Figure (14) depicts the effect of Prandtl number on secondary velocity profiles in presence of foreign species such as Mercury ($Pr = 0.025$), Air ($Pr = 0.71$) and Water ($Pr = 7.00$) are shown in figure (14). We observe that from figure (14) the velocity is decreasing with increasing of Prandtl number (Pr). Figure (9) shows that the secondary velocity profiles against y for several values of the transpiration cooling parameter (λ). As the transpiration cooling parameter is to retard the secondary velocity.

In figure (17) we depict the effect of Prandtl number (Pr) on the temperature field. It is observed that an increase in the Prandtl number leads to decrease in the temperature field. Also, temperature field falls more rapidly for water in comparison to air and the temperature curve is exactly linear for mercury, which is more sensible towards change in temperature. From this observation it is conclude that mercury is most effective for maintaining temperature differences and can be used efficiently in the laboratory.

Air can replace mercury, the effectiveness of maintaining temperature changes are much less than mercury. However, air can be better and cheap replacement for industrial purpose. This is because, either increase of kinematic viscosity or decrease of thermal conductivity leads to increase in the value of Prandtl number (Pr). Hence temperature decreases with increasing of Prandtl number (Pr). From figure (20) depicts the temperature profiles against y for various values of transpiration cooling parameter (λ) keeping other parameters are constant. Transpiration cooling parameter is found to decrease the temperature of the flow field at all points.

Research Article

Table 1: Variation of shearing stress τ_1 and τ_2 for different values of $Gr, Gc, Sc, Pr, M, m, Ec,$ and λ

Gr	Gc	Pr	Sc	M	m	Ec	λ	τ_1	τ_2
1.0	1.0	0.71	0.22	2.0	0.5	0.001	0.5	1.1507	0.2336
2.0	1.0	0.71	0.22	2.0	0.5	0.001	0.5	1.6979	0.3404
1.0	2.0	0.71	0.22	2.0	0.5	0.001	0.5	1.7544	0.3604
1.0	1.0	7.00	0.22	2.0	0.5	0.001	0.5	0.7697	0.1404
1.0	1.0	0.71	0.60	2.0	0.5	0.001	0.5	1.1070	0.2180
1.0	1.0	0.71	0.22	4.0	0.5	0.001	0.5	0.8314	0.1908
1.0	1.0	0.71	0.22	2.0	1.0	0.001	0.5	1.2552	0.4211
1.0	1.0	0.71	0.22	2.0	0.5	0.100	0.5	1.1537	0.2345
1.0	1.0	0.71	0.22	2.0	0.5	0.001	0.5	0.9824	0.1208
1.0	1.0	0.71	0.22	2.0	0.5	0.001	1.0	1.1482	0.2275

The effects of Transpiration cooling parameter (λ) and Schmidt number (Sc) on the concentration field are presented in figures (20) and (21). Figure (21) shows the concentration field due to variation in Schmidt number (Sc) for the gasses Hydrogen, Helium, Water – vapour, Oxygen and Ammonia. It is observed that concentration field is steadily for Hydrogen and falls rapidly for Oxygen and Ammonia in comparison to Water – vapour. Thus Hydrogen can be used for maintaining effective concentration field and Water – vapour can be used for maintaining normal concentration field. Figure (20) shows the plot of concentration distribution against y for different values of transpiration cooling parameter (λ) and fixed $Sc = 0.22$.

Table 2: Comparison of present Skin – friction results (τ_1) with the Skin – friction results (τ_1^*) obtained by Sriramulu *et al.*, (2007) for different values of Gr, Gc, Sc, Pr, M, m and λ

Gr	Gc	Pr	Sc	M	m	λ	τ_1	τ_1^*
1.0	1.0	0.71	0.22	2.0	0.5	0.5	1.1472	1.1469
2.0	1.0	0.71	0.22	2.0	0.5	0.5	1.4361	1.4353
1.0	2.0	0.71	0.22	2.0	0.5	0.5	1.6958	1.6941
1.0	1.0	7.00	0.22	2.0	0.5	0.5	0.6381	0.6365
1.0	1.0	0.71	0.60	2.0	0.5	0.5	1.0736	1.0725
1.0	1.0	0.71	0.22	4.0	0.5	0.5	0.7694	0.7685
1.0	1.0	0.71	0.22	2.0	1.0	0.5	1.2419	1.2410
1.0	1.0	0.71	0.22	2.0	0.5	0.5	1.1503	1.1501
1.0	1.0	0.71	0.22	2.0	0.5	1.0	1.1403	1.1395

Research Article

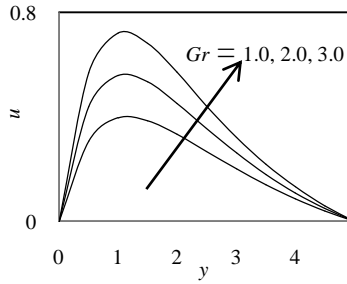


Figure 1: Effect of Grashof number Gr on primary velocity profiles u

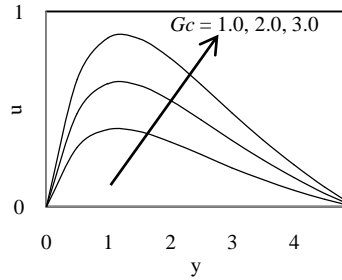


Figure 2: Effect of Modified Grashof number Gc on primary velocity profiles u

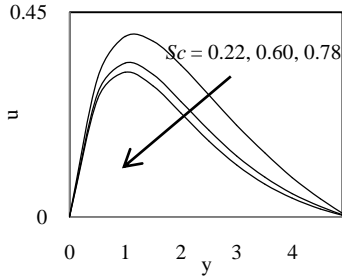


Figure 3: Effect of Schmidt number Sc on primary velocity profiles u

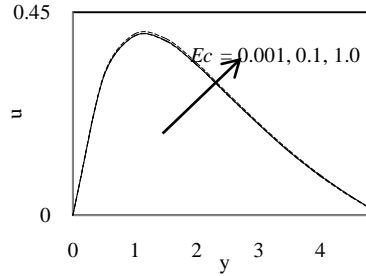


Figure 4: Effect of Eckert number Ec on primary velocity profiles u

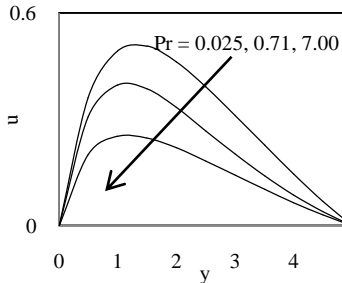


Figure 5: Effect of Prandtl number Pr on primary velocity profiles u

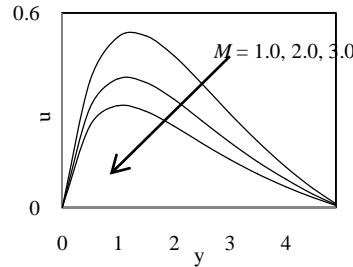


Figure 6: Effect of Hartmann number M on primary velocity profiles u

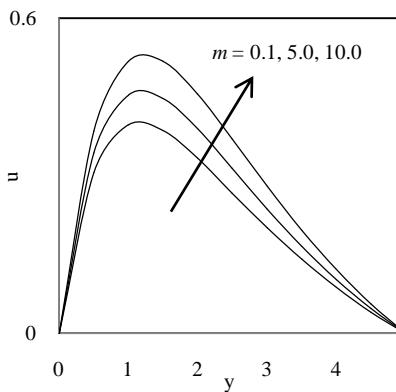


Figure 7: Effect of Hall parameter m on primary velocity profiles u

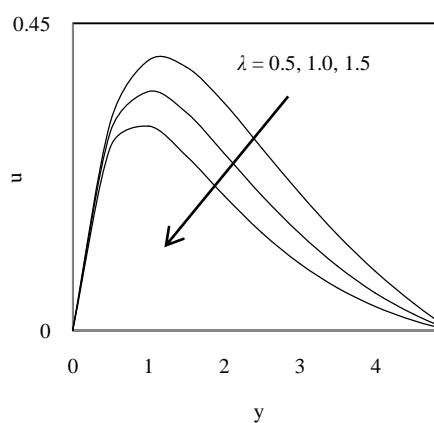


Figure 8: Effect of Transpiration cooling parameter λ on primary velocity profiles u

Research Article

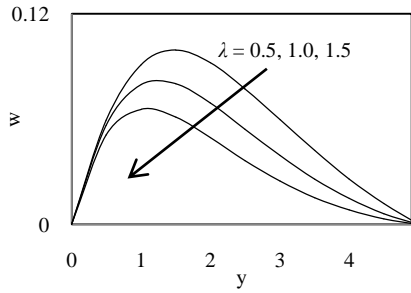


Figure 9: Effect of λ on secondary velocity profiles w

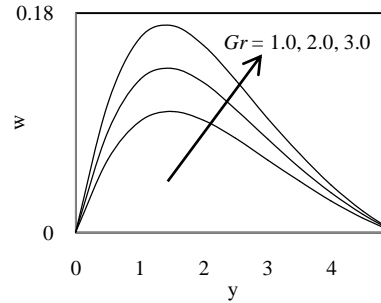


Figure 10: Effect of Grashof number Gr on secondary velocity profiles w

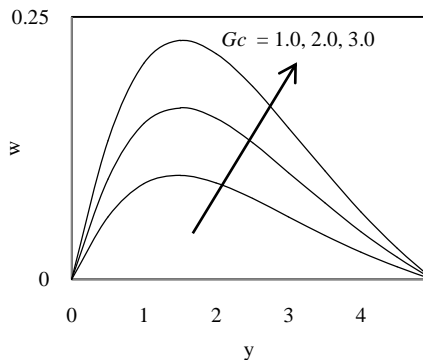


Figure 11: Effect of Modified Grashof number Gc on secondary velocity profiles w

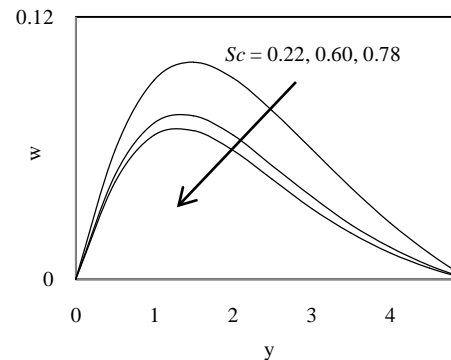


Figure 12: Effect of Schmidt number Sc on secondary velocity profiles w

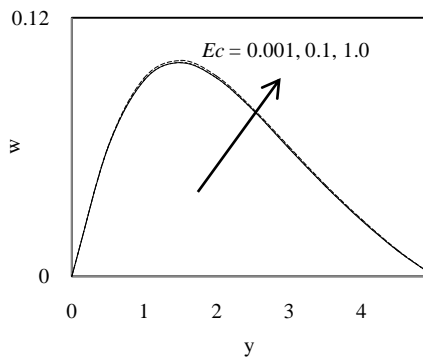


Figure 13: Effect of Eckert number Ec on secondary velocity profiles w

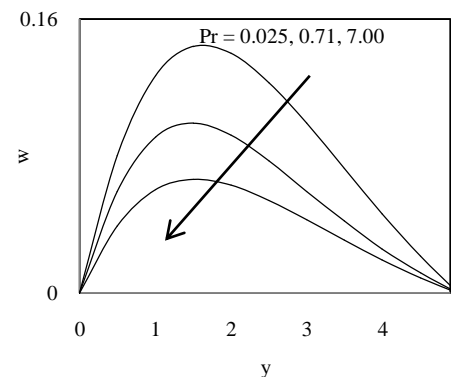


Figure 14: Effect of Prandtl number Pr on secondary velocity profiles w

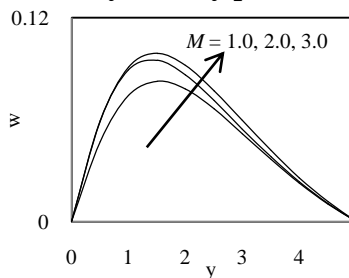


Figure 15: Effect of Hartmann number M on secondary velocity profiles w

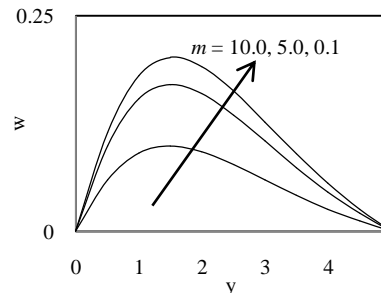


Figure 16: Effect of Hall parameter m on secondary velocity profiles w

Research Article

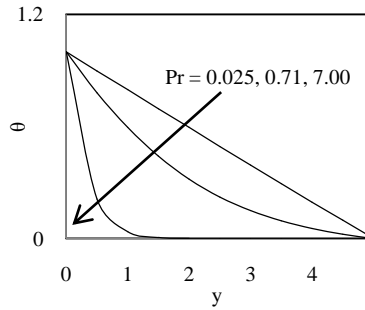


Figure 17: Effect of Prandtl number Pr on temperature profiles θ

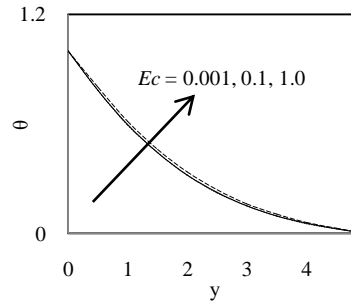


Figure 18: Effect of Eckert number Ec on temperature profiles θ

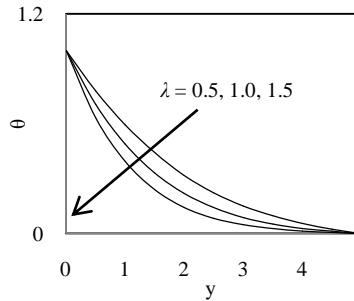


Figure 19: Effect of Transpiration cooling parameter λ on temperature profiles θ

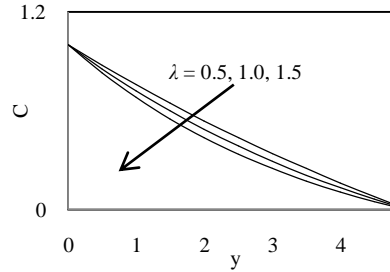


Figure 20. Effect of Transpiration cooling parameter λ on concentration profiles C

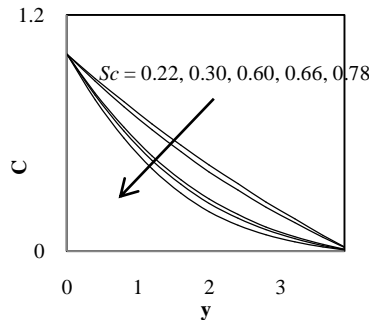


Figure 21: Effect of Schmidt number Sc on concentration profiles C

A comparative study of the curves of the above figure shows that the concentration distribution of the flow field decreases faster as the transpiration cooling parameter (λ) becomes larger. Thus greater transpiration cooling leads to a faster decrease in concentration of the flow field.

Table (1) shows the variation of different values Gr , Gc , Sc , Pr , M , m , Ec , and λ . From this table it is concluded that the magnitude of shearing stress τ_1 and τ_2 increase as the value of Gr , Gc , m , Ec increase and this behavior is found just reverse with the increase of Pr , Sc , M , λ . In order to ascertain the accuracy of the numerical results, the present skin – friction (τ_1) results are compared with the previous skin – friction (τ_1^*) results of Sriramulu *et al.*, (2007) in table 2. They are found to be in an excellent agreement.

Conclusion

The problem “The effect of Hall current on unsteady MHD flow of an electrically conducting incompressible fluid along a porous flat plate with viscous dissipation and heat absorption” is studied. The dimensionless equations are solved by using Galerkin finite element method. The Effects of primary

Research Article

velocity, secondary velocity, temperature and concentration for different parameters like Gr , Gc , Pr , Sc , M , m , λ , and Ec are studied. The study concludes the following results.

- 1). It is observed that both the primary (u) and secondary (w) velocities of the fluid increases with the increasing of parameters Gr , Gc , m , Ec and decreases with the increasing of parameters Pr , M , Sc and λ .
- 2). The fluid temperature increases with the increasing of Ec and decreases with the increasing of Pr , and λ .
- 3). The Concentration of the fluid decreases with the increasing of λ and Sc .
- 4). From table (1) it is concluded that the magnitude of shearing stress τ_1 and τ_2 increases as the increasing values of Gr , Gc , m , Ec and this behavior is found just reverse with the increasing of Pr , Sc , M , and λ .
- 5). On comparing the skin – friction (τ_1) results with the skin – friction (τ_1^*) results of Sriramulu *et al.*, (2007) it can be seen that they agree very well.

REFERENCES

- Abdul Maleque Kh and Abdur Sattar Md (2005)**. The Effects of Variable properties and Hall current on steady MHD laminar convective fluid flow due to a porous rotating disk. *International Journal of Heat and Mass Transfer* **48** 4460 – 4466.
- Ajay Kumar Singh (2003)**. MHD Free – convection and Mass Transfer Flow with Hall Current Viscous Dissipation, Joule Heating and Thermal Diffusion, *Indian Journal of Pure and Applied Physics* **41** 24 – 35.
- Anand Rao J and Srinivasa Raju R (2010)**. Applied Magnetic Field on Transient Free Convective Flow of an Incompressible Viscous Dissipative Fluid in a Vertical Channel, *Journal of Energy, Heat and Mass Transfer* **33** 313 – 332.
- Anand Rao J and Srinivasa Raju R (2011)**. Hall Effect on an unsteady MHD flow and heat transfer along a porous flat plate with mass transfer and viscous dissipation, *Journal of Energy, Heat and Mass Transfer* **32** 265 – 277.
- Anjali Devi SP, Shailendhra K and Hemamalini PT (2011)**. Pulsated convective MHD flow with Hall current, heat source and viscous dissipation along a vertical porous plate, *International Journal of Applied Mathematics and Computation* **3**(2) 141–150.
- Atul Kumar Singh, Ajay Kumar Singh and Singh NP (2005)**. Hydromagnetic free convection and Mass transfer flow with Joule heating, thermal diffusion, Heat source and Hall current, *Bulletin of the Institute of Mathematics Academia Sinica* **33**(3) 291 – 310.
- Chowdhary RC and Kumar Jha A (2008)**. Heat and mass transfer in elasticoviscous fluid past an impulsively started infinite vertical plate with Hall Effect, *Latin American Applied Research* **38** 17 – 26.
- Chaudhary RC and Jain P (2007)**. Hall Effect on MHD mixed convection flow of a Viscoelastic fluid past an infinite vertical porous plate with mass transfer and radiation, *Ukrainian Journal of Physics* **52**(10).
- Emmanuel Osalusi, Jonathan Side, Robert Harris and Barry Johnston (2009)**. On the Effectiveness of Viscous Dissipation and Joule Heating on Steady MHD and Slip flow of a Bingham fluid over a porous rotating disk in the presence of Hall and ion-slip Currents, *Romanian Reports in Physics* **61**(1) 71 – 93.
- Hossain MA and Rashid RIMA (1987)**. Hall effects on Hydro magnetic Free Convection Flow along a Porous Flat Plate with Mass Transfer, *Journal of the Physical Society of Japan* **56** 97 – 104.
- Palumbo LJ and Platzeck AM (2006)**. MHD stationary symmetric flows with Hall effect, *Journal of Plasma Physics* **72** 457-467

Research Article

Rajashekhar MN, Anand Rao J and Shanker B (1999). Numerical Solutions of Hall Effects on Heat and Mass Transfer Flow through Porous Medium, *Journal of Energy Heat and Mass Transfer* **21** 1 – 7.

Singh NP (1996). Mass Transfer effects on the Flow Past a vertical Porous Plate, *Proceedings of the American Mathematical Society* **12** 109 – 114.

Singh NP, Singh AK and Kumar R (1996). Free Convection Heat and Mass Transfer along a Vertical Surface in a Porous Medium, *Indian Journal of Theoretical Physics* **44** 255 – 264.

Soundalgekar VM, Ray SN and Dass VN (1995). Coupled Heat and Mass transfer by Natural Convection from Vertical Surfaces in Porous Medium, *Proceedings of the American Mathematical Society* **11** 95 – 98.

Srihari K, Kishan N and Anand Rao J (2008). Hall Effect on MHD Flow and Heat Transfer along a Porous Flat Plate with Mass Transfer and Source/Sink, *Journal of Energy, Heat and Mass Transfer* **30** 361 – 376.

Sriramulu A, Kishan N and Anand Rao J (2007). Effect of Hall Current on MHD Flow and Heat Transfer along a Porous Flat Plate with Mass Transfer, *Journal of the Institute of Engineering* **87** 24 – 27.